Int. J. Electrochem. Sci., 8 **(2013)** 5438 - 5447

International Journal of
ELECTROCHEMICAL
SCIENCE
www.electrochemsci.org

Influence of Working Frequency on Structure and Corrosion Resistance of the Anodic Oxide Film on Ti–6Al–4V Alloy

Songmei Li[*], *Xiumei Yu, Jianhua Liu, Mei Yu, Guolong Wu, Liang Wu, Kang Yang*

School of Materials Science and Engineering, Beihang University, 100191, Beijing, China
[*]E-mail: songmei_li@buaa.edu.cn

Received: 25 January 2013 / *Accepted:* 15 March 2013 / *Published:* 1 April 2013

To evaluate influence of working frequency on the structure and corrosion resistance of oxide film on Ti–6Al–4V alloy, an anodic oxidation is conducted employing direct-current (DC) pulse power source in an environmental friendly electrolyte. Scanning electron microscopy (SEM), Raman spectroscopy, and electrochemical techniques are employed to characterize the oxide film. It shows that the oxide film presents a uniform petaloid drum and micro-cracks morphology. Additionally, the micro-cracks dramatically swell with the enhancing of frequency, as well as the thickness increase of the oxide film. The Raman analysis result illustrates a close similarity in the crystal structure of the obtained Ti–6Al–4V oxide films with the increasing frequency. And the higher the working frequency, the more crystalline oxides (anatase and rutile) are. Furthermore, at the frequency of 120freq/min, a most positive corrosion potential and minimum corrosion current density are observed, demonstrating an appropriate working frequency for fabrication of the corrosion-resistant anodic oxide film.

Keywords: pulse anodic oxidation, Ti–6Al–4V, oxide film, corrosion resistance

1. INTRODUCTION

Anodic oxidation is a traditional surface modification technology, by which a compound oxide film is grown in-situ on valve-metals directly [1]. A uniform and color-bright oxide film can be fabricated on the surface of titanium and its alloy using this technology, which greatly improves its resistance to wear, adhesion and corrosion, etc.[2-4]. Therefore, anodic oxidation has been widely used in aerospace, warship, sports, medical science and other fields [5].

The anodic growth process of the oxide films reveals that their performance strongly depends on the electrical source, electrolyte and temperature. The electrolyte and temperature has already been widely studied by many researchers [6-9]. There are three basic kinds of electrical sources: direct-

current type that are used foremost, the alternating-current type and pulsed type that are widely adopted at present [1]. It is mentioned in literatures [10, 12-18, 20, 21] that anodic oxidation of titanium was carried out by using direct-current source, through which a layer of dense oxide film is produced on the surface. Furthermore, compared with alternating-current source, direct-current type is more energy-saving to achieve the uniform oxide film. Qiu etc. [10] studied the effect of different wave pattern on the anodic oxide film. Their research concluded that the resistance to corrosion and abrasion of oxide film formed by pulse direct-current was better than other wave pattern. Consequently, pulse direct-current source has obvious advantages in preparing well-structured, corrosion-resistant oxide film.

The pulse direct-current source has four pulse parameters: current density, applied potential, frequency and duty ratio. The effect of current density and applied potential on structure and property of anodic oxide film have been studied [8, 15-17]. M.V. Diamanti etc. [15] found that the voltage increases with the enhancing current density and oxide conversion to anatase is promoted by an increase in current density. Yao etc. [18] studied the influence of the frequency on the structure and corrosion resistance of ceramic coatings on Ti–6Al–4V alloy produced by micro-plasma oxidation. Until recently, there is little information available in literature about the influence of frequency on structure and corrosion resistance of the anodic oxide film fabricated in the environmental friendly electrolyte.

In our previously work, thick, uniform and non-transparent anodic oxide films were fabricated on the Ti–10V–2Fe–3Al alloy by using a pulse galvanostatic method [19]. Recently, the influence of incremental rate of anodizing current on roughness and electrochemical corrosion properties of oxide film on titanium alloy Ti–10V–2Fe–3Al were studied [20]. Besides, among Ti and its alloys, Ti–6Al–4V alloy is most widely used in many fields. Therefore, the purpose of this paper is to study the influence of working frequency on morphology, structure and corrosion resistance of the oxide film on Ti–6Al–4V by DC pulse anodic oxidation power in the new environmental friendly $C_4H_4O_6Na_2$ electrolyte.

2. EXPERIMENTAL

2.1. Preparation of the oxide film

A forged block of titanium alloy Ti–6Al–4V (88.7%Ti, 6.32%Al, 4.10%V, 0.30%Fe, 0.10%C, and 0.05% N) was cut into slices with the dimension of 1 mm×1mm×2 mm. Prior to pulse anodizing, samples were abraded with silicon carbide paper successively grades from 200 to 2000 grit and then ultrasonically cleaned in acetone solution, rinsed in de-ionized water and, finally, air dried.

Anodic oxidation was carried out using a pulse galvanostatic power source (WMY-V) in a cell with a thermostat water bath and a magnetic stirring apparatus. The output mode of the power source is shown in Fig. 1. The Ti–6Al–4V slice sample was used as anode, and a 1Cr18Ni9Ti stainless steel plate was used as cathode. The parameters of anodizing process are given in Table 1. After the

treatment, the coated samples were rinsed with water and the dried in the air. Three samples were made under each condition to ensure the accuracies of the experiments.

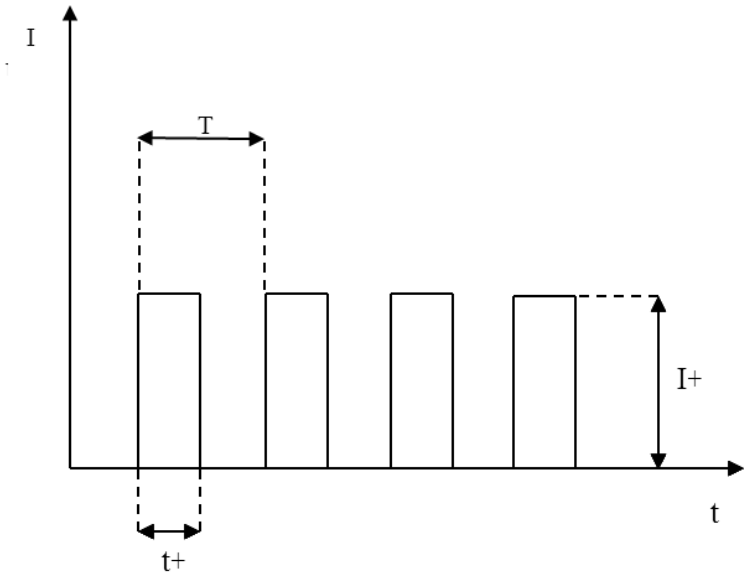

Figure 1. The output mode of power source: T pulse cycle, t+ pulse working period, I+ pulse anodic current

Table1. Parameters of fabrication process

Parameter	Value
Current density/(A•dm^{-2})	4
electrolyte concentration/(g•L^{-1})	30
Anodizing time/(min)	40
Temperature/ (℃)	18±2
Duty ratio/ (%)	20
Frequency/(freq/min)	60, 120, 240, 480

2.2. Morphology and crystal structure of the oxide film

The surface morphology, cross-section morphology and thickness of the oxide films were examined using scanning electron microscopy (SEM, Camscan CS3400). The crystalline structure of oxide films were determined by Raman spectroscopy (Raman, Yvon Jobin Horiba-HR800, He–Ne laser without filter, 650 nm).

2.3. Corrosion resistance properties

Electrochemical experiments were measured in a traditional three-electrode system (a platinum electrode as counter electrode, a Ag/AgCl as reference electrode and the oxide sample as working electrode) by using a potentiostat/galvanostat (Parstat 2273, Princeton Applied Research, USA) in a 3.5% NaCl solution. All experiments were carried out at room temperature. The scanning rate of the potentiodynamic polarisation curve was $0.5 mVs^{-1}$, with a scanning range from −0.25V to +0.25V vs the open circuit potential.

3. RESULTS AND DISCUSSIONS

3.1. Relationship among frequency, voltage, and thickness

The color and thickness of anodic oxide film depend on the anodic forming voltage [13]. Fig.2. shows voltage - time plot during the formation of anodic oxidation film at different frequencies. According to Fig.2, the film forming voltage increases as the frequency increases. The oxide film grows gradually with the increase in voltage after the electrical breakdown of the passivating film of the Ti–6Al–4V substrate. An increasing in frequency changed the character of the developing oxide film. Firstly, the interference color of the oxide film fabricated at different frequencies was different. At 60freq/min, the oxide film was caesious.

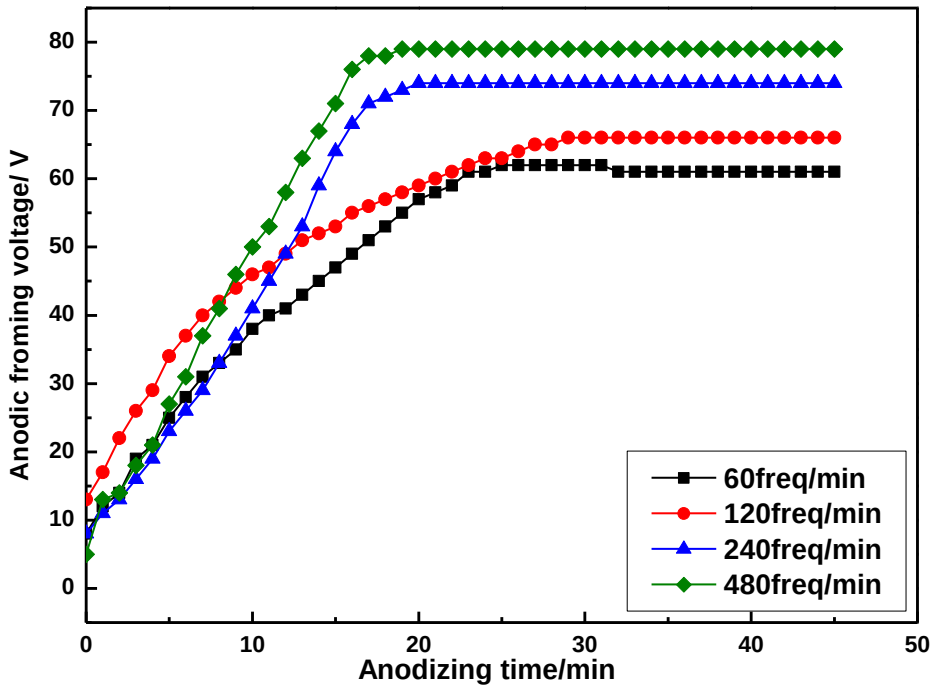

Figure 2. Anode oxidation film forming voltage - time plot at different frequencies

Table2. The thickness and ultimate voltage of the oxide film fabricated at different frequencies

Frequency /(freq/min)	Thickness(um)	Ultimate voltage
60	2.3	61
120	10.8	66
240	15.1	74
480	16.0	79

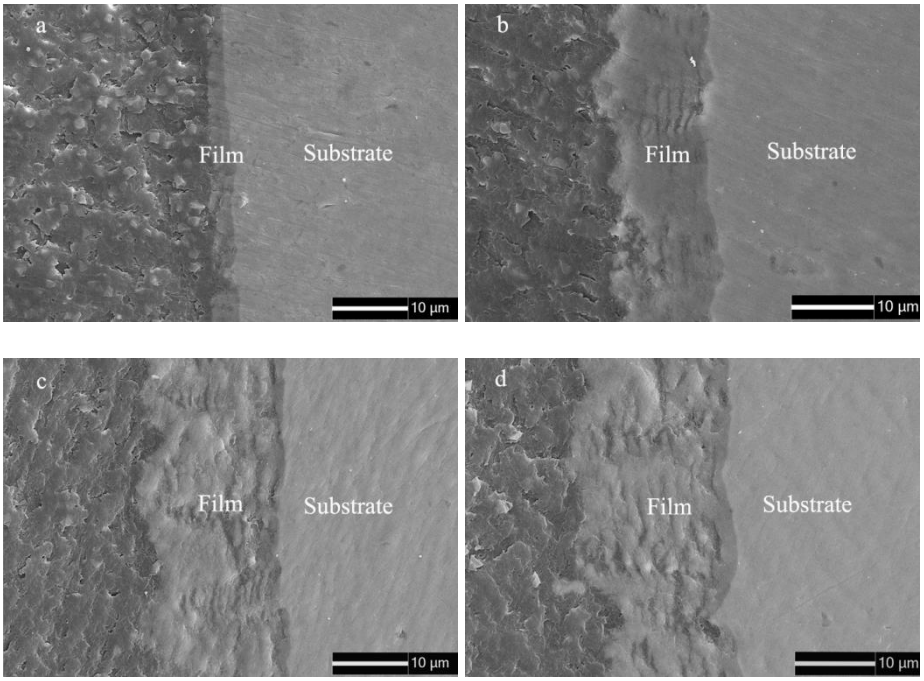

Figure 3. The cross-section images of the anodic oxide films fabricated at different frequencies: (a) 60freq/min; (b) 120freq/min; (c) 240freq/min; (d) 480freq/min

With increasing frequency, the oxide film turned to yellow. Secondly, the frequency also influenced the ultimate voltage and thickness of the produced oxide film, which are presented in Fig.2 and table2, respectively. Both the ultimate voltage and thickness of the oxide film increased with increasing frequency. These indicate that the higher the ultimate voltage, the thicker the oxide film is.

Fig.3 presents the cross-section images of the anodic oxide film fabricated at different frequencies. The thickness of the oxide films increases as the frequency enhances. According to previous study, the anodic oxide film can be divided into two layers: a loose outer layer and a barrier inner layer [13]. It is more distinct as shown in Fig.3 (d). It's perceptible that the oxide layer became increasingly loose when the frequency exceeded 120freq/min.

Generally speaking, it is assumed that the growth of anodic oxide film is characterized by the electrochemical dynamics between the oxide film formation rate and the oxide dissolution rate.

According to Fig.2, the anodizing process can classified into two steps: in the first step (step1), the anodizing voltage increased linearly with time up to the maximum anodizing voltage; in the second step (step2), the anodizing voltage approximately maintained at a steady value. In step1, the rate of oxide film formation overwhelmingly exceeded the rate of chemical dissolution. As a result, the oxide thickness and voltage increase rapidly. In step2, a dynamic equilibrium between oxide formation and chemical dissolution is established and might be related to the thickness of the outer loose layer. Comparing with the other curves, at the frequency of 120freq/min, the increase rate of the step 1 is the slowest which is more conducive to the growth of the compact oxide layer. However, at the frequency of 240freq/min and 480freq/min, the duration of the step 2 is longer than the other two which lead to the formation of the loose oxide layer. Therefore, the oxide layer became increasingly loose when the frequency exceeded 120freq/min. Stated thus, it seems that at the frequency of 120freq/min, the oxide film owns best compactness and proper thickness attained in the anodizing sample.

3.2 Morphology of the oxide film

The SEM morphology of anodic film fabricated at different frequencies is shown in Fig 4. Fig 4 (a) indicates the presence of electron transport channels appearing as circular spots distributed over the surface of the oxide film when the frequency is 60 freq/min. However，the electron transport channels are almost covered when the frequency enhances to 120freq/min, instead, it translates to petaloid drums. With the enhancing of frequency, on one hand, the size of the petaloid drums increases; on the other hand, the micro-cracks are dramatically swelling.

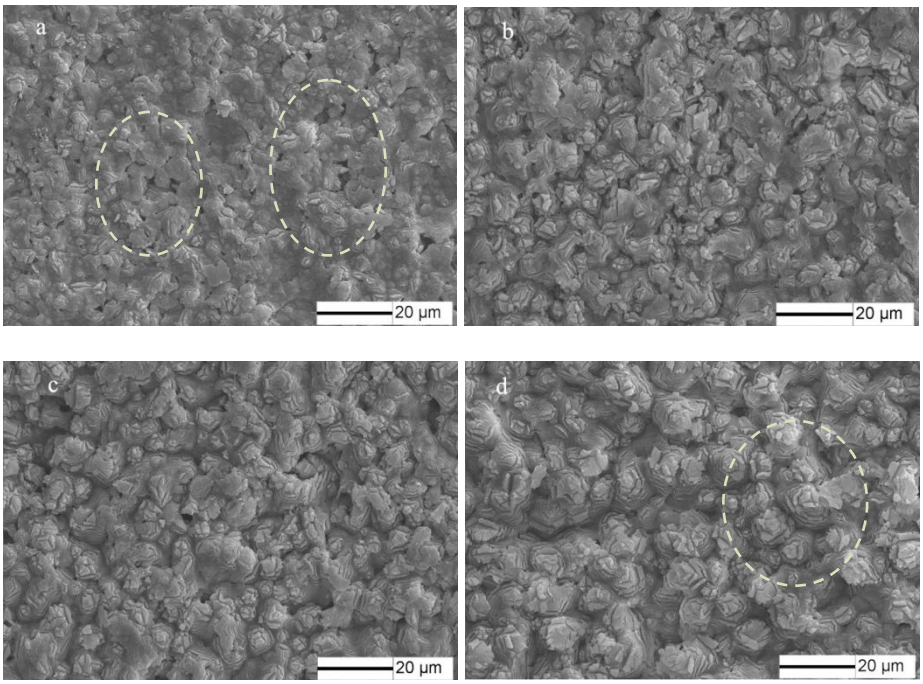

Figure 4. SEM morphologies of pulse anodic film fabricated at different frequencies: (a)60freq/min; (b)120freq/min; (c)240freq/min; (d)480freq/min

The working frequency is one of the most important parameters for the DC pulse anodic oxidation process. According to Fig.1, one pulse cycle of the electrical source includes a pulse working period and a dead time. A change of frequency essentially influences the action duration and the action times within one unit of time. An increase of the working frequency leads to more interruptions of anodic oxidation process by the dead time, and the action duration of the anodic oxidation process is shortened [18].

At low frequencies, the pulse cycle is long, which leads to the reaction heat failed to be taken away and thus affects the film growth [21]. According to Fig.2, the film forming voltage increases as the frequency enhances. The evolution of oxygen generates surface defects and electron transport channels i.e. micro-holes in Fig. 4(a) when it achieves the breakdown voltage [13].

As the frequency enhances, the number of pulse dead times increased [19]. It is possible for the reaction heat to be taken away the on time. It makes the thickness of oxide film increases with enhancing frequency (Fig. 3(b)). Meanwhile, the electron transport channels are almost covered with the drums. The drums distribute almost uniforms on the surface and connect to each other when the frequency reaches to120 freq/min.

When the frequency continues to increase, the anodizing voltage increases and residual reaction heat within per unit time raises. In the case of the high voltage and temperature locally, the petaloid drums grow and extrude, which yields the compression stress. Subsequently, the micro-cracks are dramatically swelling. Therefore, the loose layer of the oxide film is produced gradually (Fig. 3(c) (d)), that is, the oxide layer became increasingly loose when the frequency exceeded 120freq/min. It brings into correspondence with the above analysis.

3.3 Crystalline structure

The Raman spectra of the oxide film fabricated at different frequencies is shown in Fig.5. Rutile has three intense Raman active fundamentals (224, 446, 612cm^{-1}) [22], while anatase has five Raman active fundamentals (144, 198, 399, 516, 639 cm^{-1}) [23]. The band at 144 cm^{-1} is very intense and sharp. It is assigned to the vibrational mode with Eg symmetry. Another obvious intense band of the oxide films was detected at 612 cm^{-1} and assigned to the B_{1g} vibrational mode. Other vibrational modes were observed at 504–516 cm^{-1}(B_{1g}).It is apparent that the oxide film fabricated at different frequency has the same peaks. On the other hand, the intensity increases with an enhancing in working frequency. Consequently, the films have the same crystal structure (anatase and rutile), well the intensity of TiO_2 anatase and TiO_2 rutile increase with the enhancing of frequency.

The crystal structure of the anodic oxide films can be explained by the ultimate voltage. In general, at low applied voltages, the anodic oxide film is amorphous [20]. With increasing voltages, the structure of the oxide film changes from amorphous to crystalline. Hence, the higher the working frequency, the higher the ultimate voltage is and the more crystalline oxides (anatase and rutile) are. The intensity of the peaks corresponds to the ultimate voltage value.

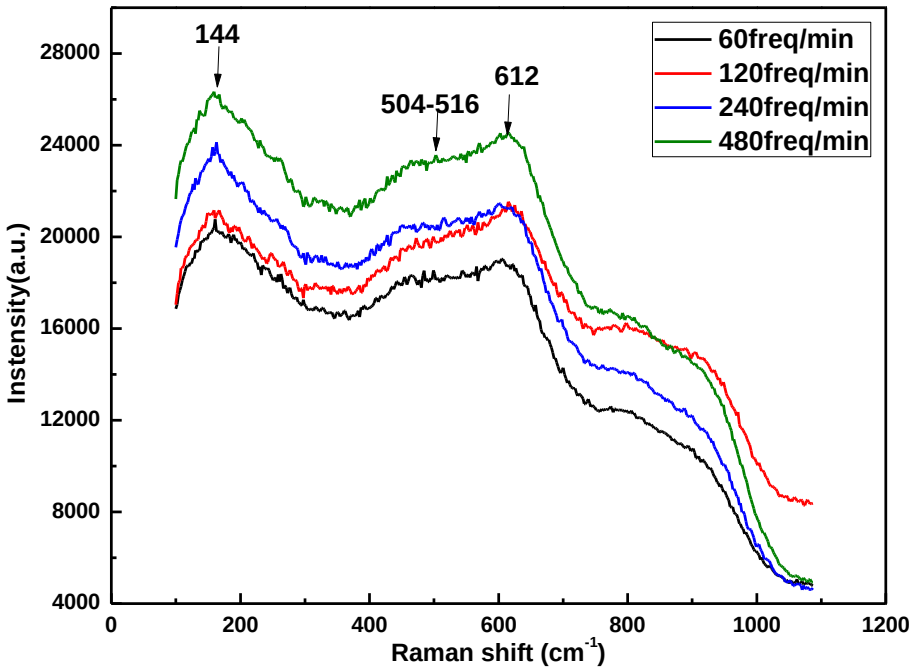

Figure 5. Raman spectra of the anodic oxide films fabricated at different frequencies

3.4 Corrosion resistance

Fig. 6 shows polarizing curves of the anodic oxide films in a 3.5% NaCl solution. The detailed data are given in Table 3. Results present that the anodic oxidation shifted the electrode potential of Ti–6Al–4V from negative to positive, and reached the maximum at 120freq/min.

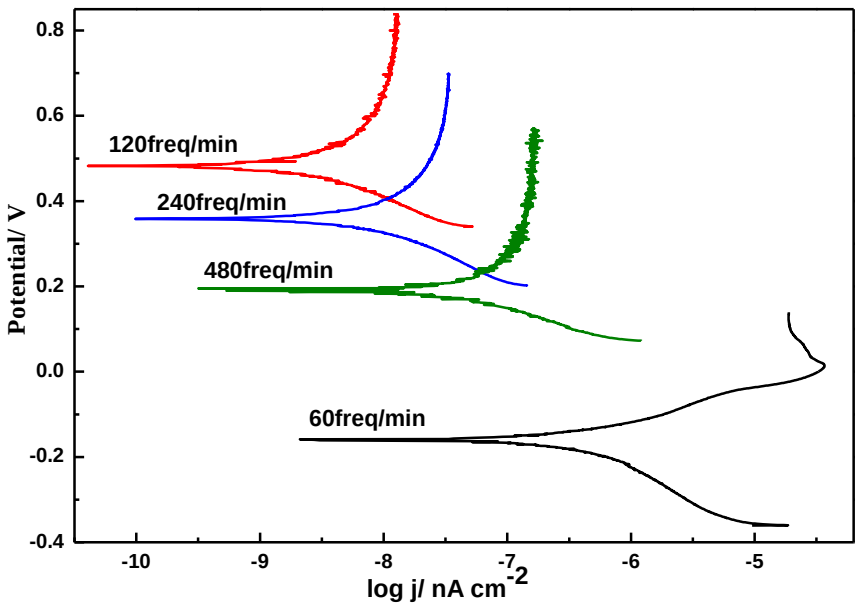

Figure 6. Polarizing curves of the anodic oxide film fabricated at different frequencies

Table3. Properties of anodic oxide films fabricated at different frequencies

频率/(freq/min)	E_{corr} /V	i_{corr} /(uA•cm^{-2})
60	—0.162	3.443×10^{-7}
120	0.482	7.830×10^{-9}
240	0.358	1.965×10^{-8}
480	0.195	1.290×10^{-7}

Similarly, the corrosion current density i_{corr} of the anodic oxide films decreased with a decrease in frequencies before 120freq/min, and then increased with further decrease of the frequency. Therefore, the appropriate frequency is 120freq/min for fabricating corrosion-resistant anodic oxide film.

According to polarizing curves and Table 3, the anodic oxidation potential processing shifted shifts the E_{corr} from negative to positive as the frequency enhances, and reaches the maximum at 120freq/min. Similarly, the corrosion current density i_{corr} of the anodic oxide films decreases with a decrease in frequency before 120freq/min, and then increases with further decrease of the frequency. In general, the corrosion resistance of the anodizing samples is mainly associated with the thickness, the surface state of the oxide films and the composition as well [18]. As all the anodic oxide films have the same crystal structure (anatase and rutile) in the experiment, the key factors would then be mainly attributed to the thickness and the surface state. However, according to Fig.3 and the previous analyses, there seems to be a conflict between the thickness and the compactness of the oxide films at different frequencies: the thicker the oxide films, the worse the compactness. According to the results of electrochemical measurement, the obtained oxide films had best corrosion resistance when the frequency is fixed at 120freq/min. Therefore, the appropriate frequency is 120freq/min for fabricating well-structured, corrosion-resistant anodic oxide film.

4. CONCLUSIONS

The influence of the working frequency on the morphology, structure and corrosion resistance of oxide film on Ti–6Al–4V by DC pulse anodic oxidation power in the new environmental friendly $C_4H_4O_6Na_2$ electrolyte has been studied in this work, and the following conclusions are obtained.

(1) The anodizing process can classified into two steps: in the first step (step1), the anodizing voltage increased linearly with time up to the maximum anodizing voltage; in the second step (step2), the anodizing voltage approximately maintained at a steady value.

(2) The oxide film presents uniform petaloid drums morphology. With the enhancing of frequency, these petaloid drums grow and extrude, which yields the compression stress. Subsequently, the micro-cracks are dramatically swelling.

(3) The thickness of the oxide film increases as the frequency increased. The oxide layer became increasingly loose when the frequency exceeded 120freq/min. The oxide films fabricated at frequency of 120freq/min is relative compact.

(4) Raman spectroscopy analysis illustrates that the films have the same crystal structure (anatase and rutile), well the intensity of TiO_2 anatase and TiO_2 rutile increase with the enhancing of frequency.

(5) The anodic oxidation processing shifts the E_{corr} from negative to positive as the frequency enhances, and reaches a maximum at 120freq/min. Similarly, it illustrates a minimum corrosion current density.

Consequently, the appropriate frequency is 120freq/min for fabricating well-structured, corrosion-resistant anodic oxide film.

ACKNOWLEDGEMENT
This work is supported by the National Natural Science Foundation of China (No. 51271012).

References

1. A. Aladjem, *J. Mater. Sci.,* 8 (1973) 688,788-790.
2. D. Capek, M-P.Gigandet, M. Masmoudi, M. Wery and O. Banakh, *Surf. Coat. Tech.,* 202 (2008) 1383.
3. S. Kumar, T.S.N. S. Narayanan, S. G. S. Raman and S.K. Seshadri, *Mat. Sci. Eng*. C 30 (2010) 926.
4. M. P. Neupane1, Il S. Park, S. J. Lee, K. A. Kim, M. H. Lee and T. S. Bae, *Int. J. Electrochem. Sci.,* 4 (2009) 198.
5. S. Tanaka, N. Hirose and T. Tanakic , *J. Electrochem. Soc.*, 152 (2005) C789.
6. J. H. Liu, J. L. Yi, S. M. Li, M. Yu, G. L. Wu and L. Wu, *J. Appl. Electrochem*., 40 (2010) 1546.
7. G. A. EL-Mahdy, *Corrosion,* 63 (2007) 303.
8. S. Kaneco, Y.S. Chen, P. Westerhoff and J. C. Crittenden, *Scripta. Mater.*, 56 (2007) 374.
9. T. Ohtsuka, M. Masuda and N. Sato, *J. Electrochem. Soc*., 132 (1985) 788.
10. W. Simka, *Electrochim. Acta*, 56 (2011) 9832.
11. Il S. Park, T. G. Woo, W. Y. Jeon and H. H. Park, *Electrochim. Acta*, 53 (2007) 864.
12. S.K. Poznyak, A. D. Lisenkov, M.G.S. Ferreiraa, A.I. Kulakc and M.L. Zheludkevicha, *Electrochim. Acta*, 76 (2012) 455.
13. J. L. Yi, J. H. Liu, S. M. Li, M. Yu, G. L. Wu and L. Wu, *J. Cent. South Univ. Technol*., 18 (2011) 7, 13.
14. Y. Yin and W. B. Qiu, *Mater. Mech. Eng*., 29 (2005) 36.
15. M. V. Diamanti and M. P. Pedeferri, *Corros. Sci*., 49 (2007) 948.
16. II S. Park, M. H. Lee, T. S. Bae and K.W. Seol, *J. Biomed. Mater. Res*. B, 10 (2007) 422.
17. N. K. Kuromoto, R. A. Simão and G. A. Soares, *Mater. Charact.,* 58 (2007) 114.
18. Zh. P. Yao, Zh. H. Jiang, X. T. Sun, Sh. G. Xin and Zh. D. Wu, *Mater. Chem. Phys*., 92 (2005) 411.
19. J. H. Liu, J. L. Yi, S. M. Li, M. Yu and Y. Z. Xu, *Int. J. Min. Met. Mater.*, 16 (2009) 96.
20. J. H. Liu, G. L. Wu, M. Yu, L. Wu, Y. Zhang and S. M. Li, *Sur. Eng.*, 28 (2012) 406.
21. H. H. Zhou, W. Deng, Zh. Z. Chen, Ch.Y. Peng and Y. F. Kuang, *Plat. Eng*., 26 (2004) 3.
22. S. P. S. Porto, P. A. Fleury and T. C. Damen, *Phy. Rev*. B., 154 (1967) 523.
23. T. Ohsaka, F. Izumi and Y. Fujiki, *J. Raman. Spectrosc*., 7 (1978) 322.